ADVANCED MATERIALS
www.advmat.de

Materials Views
www.MaterialsViews.com

Flexible Low-Voltage Organic Transistors and Circuits Based on a High-Mobility Organic Semiconductor with Good Air Stability

By *Ute Zschieschang,* Frederik Ante, Tatsuya Yamamoto, Kazuo Takimiya, Hirokazu Kuwabara, Masaaki Ikeda, Tsuyoshi Sekitani, Takao Someya, Klaus Kern,* and *Hagen Klauk*

When organic thin-film transistors (TFTs) are exposed to air, the electrical performance of the devices often degrades over time. The degradation is often the result of the oxidation of the conjugated molecules in the presence of oxygen, water vapor, or ozone. Oxidation changes the energies of the molecular orbitals and thereby affects the charge carrier transport. For example, when pentacene is oxidized, the hydrogen atoms at the central aromatic ring of the molecule are replaced with oxygen, forming 6,13-pentacenequinone.[1] Unlike hydrogen, oxygen is linked to the carbon atoms via double bonds, so the oxidation leads to the loss of conjugation at the central ring. Oxidizing pentacene therefore reduces the extent of the conjugated π-system from five rings to four rings, which in turn causes an increase in the highest occupied molecular orbital (HOMO) energy.[2,3] Due to the difference in energy between the HOMO of pentacene and the HOMO of 6,13-pentacenequinone, charge carriers are not easily exchanged between the two molecules, so the quinone molecules do not participate in the transport of charge carriers through the film. Also, because the quinone molecules have a different shape than the pentacene molecules, they produce distortions in the pentacene lattice that become scattering sites.[4] As more and more pentacene molecules are oxidized, the carrier mobility therefore decreases over time.[5–8]

[*] Dr. U. Zschieschang, F. Ante, Prof. K. Kern, Dr. H. Klauk
Max Planck Institute for Solid State Research
Heisenbergstr. 1, 70569 Stuttgart (Germany)
E-mail: u.zschieschang@fkf.mpg.de
Dr. T. Yamamoto, Prof. K. Takimiya
Department of Applied Chemistry, Graduate School of Engineering
Institute for Advanced Materials Research, Hiroshima University
Higashi-Hiroshima (Japan)
Dr. H. Kuwabara, Dr. M. Ikeda
Functional Chemicals R&D Laboratories
Nippon Kayaku Co., Ltd.
Kita-ku, Tokyo (Japan)
Dr. T. Sekitani, Prof. T. Someya
Department of Electrical Engineering, University of Tokyo
Tokyo (Japan)
Prof. K. Kern
Institut de Physique de la Matière Condensée
Ecole Polytechnique Fédérale de Lausanne (Switzerland)

DOI: 10.1002/adma.200902740

One strategy to improve the air stability of organic TFTs is to employ a semiconductor that is less easily oxidized, that is, a molecule with a larger ionization potential.[9–15] However, most TFTs based on organic semiconductors with large ionization potential show mobilities smaller than that of pentacene (i.e., below about 1 $cm^2\ V^{-1}\ s^{-1}$), most likely due to a thin-film microstructure that is less favorable in terms of orbital overlap and efficient charge transfer. Exceptions include di(phenylvinyl)anthracene (DPVAnt) with an ionization potential of 5.4 eV, a mobility of 1.3 $cm^2\ V^{-1}\ s^{-1}$, and good air stability.[16,17] Another promising class of air-stable conjugated semiconductors are the derivatives of benzothienobenzothiophene (BTBT), which are also characterized by excellent thin-film microstructures, large hole mobilities, and large ionization potentials (between 5.4 to 5.7 eV).[18–21] For one of these materials, dinaphtho-[2,3-b:2′,3′-f]thieno[3,2-b]thiophene (DNTT), Yamamoto and Takimiya recently reported a mobility of 2.9 $cm^2\ V^{-1}\ s^{-1}$ and good air stability for TFTs fabricated on octadecyltrichlorosilane (OTS)-functionalized Si/SiO_2 substrates.[22] Here we report on the performance and stability of low-voltage DNTT TFTs, inverters, and ring oscillators on flexible polymeric substrates.

DNTT was synthesized in three steps involving the selective functionalization of commercially available 2-naphthaldehyde with methylthio substituents by ortho-directing lithiation, a low-valence titanium-mediated McMurry coupling reaction, and a ring-closing reaction with excess iodine.[22] The product was purified by temperature-gradient sublimation in a stream of inert gas. The HOMO energy of DNTT determined by cyclic voltammetry is −5.4 eV (compared to −5.0 eV for pentacene[17]) and the optical bandgap estimated from UV–Vis absorption spectroscopy is 3.0 eV (compared with 1.8 eV for pentacene[17]).

Transistors and circuits were prepared on 125-μm-thick flexible polyethylene naphthalate (PEN) film (Teonex Q65; kindly provided by William A. MacDonald, DuPont Teijin Films, Wilton, UK). Aluminum (20-nm-thick) was deposited through a shadow mask to define the gate electrodes. The aluminum was briefly exposed to an oxygen plasma to create a 3.6-nm-thick aluminum oxide layer. The substrate was then immersed in a 2-propanol solution of n-tetradecylphosphonic acid to form a 1.7-nm-thick self-assembled monolayer (SAM) on the surface of the oxidized gates. Thus, the AlO_x/SAM gate dielectric has a total thickness of 5.3 nm and a capacitance of 800 nF cm^{-2}, which allows the devices and circuits to operate with voltages of 3 V. A 30-nm-thick

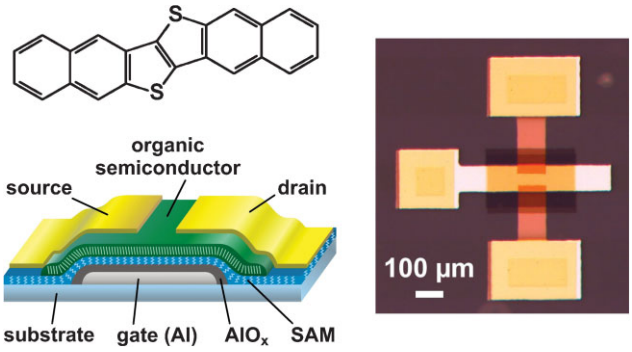

Figure 1. Cross section and photograph of a DNTT TFT on a flexible PEN substrate. The chemical structure of the organic semiconductor DNTT is also shown.

film of DNTT was then deposited through a shadow mask by sublimation in a vacuum evaporator, followed by the deposition of 30-nm-thick gold through another shadow mask to define the source/drain contacts. Figure 1 shows the schematic TFT structure and a photograph of a completed device. Vias for reliable electrical contact between the gate level and the source/drain level were defined by a simple process that exploits the surface selectivity of the self-assembling phosphonic acid molecules during the adsorption process.[23] The maximum temperature during the transistor and circuit manufacturing process was 60 °C, which is the substrate temperature during the DNTT deposition. All electrical measurements were performed in ambient air at room temperature.

Figure 2a shows the current–voltage characteristics of a DNTT TFT on a flexible PEN substrate recorded in air shortly after device fabrication. The TFT has a mobility of 0.6 $cm^2 V^{-1} s^{-1}$, an on/off current ratio of 10^6, and a subthreshold swing of 100 mV per decade. Figure 2b shows the electrical characteristics of the same transistor after the substrate had been exposed to ambient air with a humidity of about 50% and yellow laboratory light for a period of 8 months (246 days). The aged device has a mobility of 0.3 $cm^2 V^{-1} s^{-1}$, an on/off ratio of 10^6, and a subthreshold swing of 150 mV per decade. The results in Figure 2 show that after 8 months of continuous exposure to air and light the carrier mobility of the DNTT TFT is still 50% of its initial value. For comparison, the mobility of pentacene TFTs manufactured using the same technology decreased by more than an order of magnitude after just 3 months in air. Thus, the larger ionization potential of DNTT (5.4 eV) compared with that of pentacene (5.0 eV) provides a dramatic improvement in the air stability of the transistors. To obtain organic TFTs with even better air stability it may be necessary to synthesize conjugated molecules with an even larger ionization potential (perhaps approaching 6 eV) and with a similar thin-film microstructure (and hence large carrier mobility). However, such a large ionization potential inevitably creates a significant energy barrier at the source and drain contacts that may lead to excessive contact resistance.[17]

When a carrier channel is created in a field-effect transistor by applying a gate–source voltage, the number of mobile carriers in the channel decreases over time as more and more of the carriers are trapped into localized electronic states. This is known as bias stress effect and manifests itself as a time-dependent decrease in

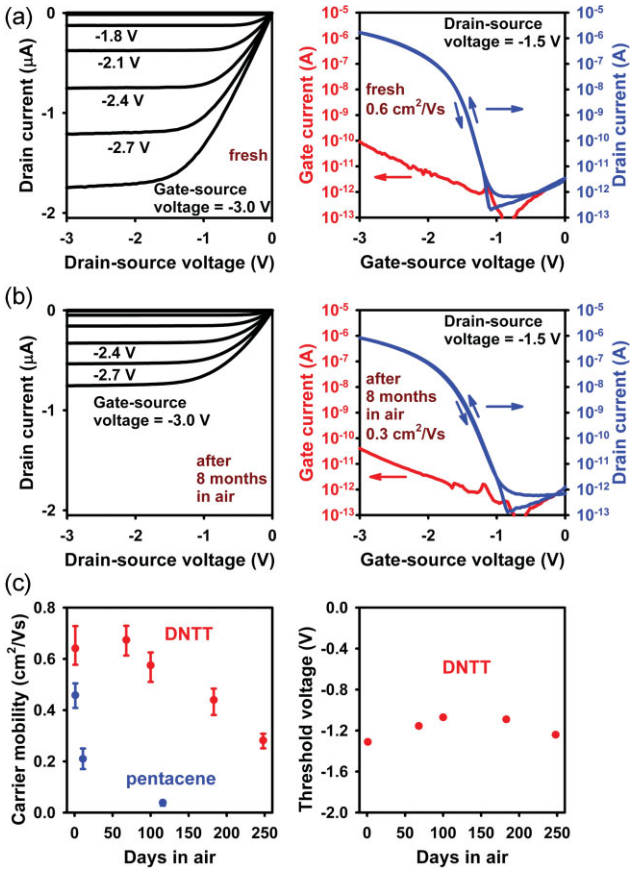

Figure 2. Current–voltage characteristics of a DNTT TFT on a flexible PEN substrate. a) Transistor characteristics recorded shortly after device fabrication. b) Transistor characteristics recorded after 8 months in air. c) Carrier mobility and V_{th} over time. (For comparison, the mobility of a pentacene TFT based on the same technology is also shown.) The TFT has a channel length of 30 µm and a channel width of 100 µm.

drain current and a shift in threshold voltage (V_{th}).[24–27] The physical location and energy of the trap sites, the trapping and release kinetics, and the rate of the V_{th} shift depend on the materials employed for the semiconductor and the gate dielectric[26] and on the electric field during bias stress.[27] For pentacene TFTs with an AlO_x/SAM gate dielectric similar to the one utilized here, a V_{th} shift of 0.3 V after 24 h of continuous stressing with a gate–source voltage of −3 V (corresponding to a gate field of about 5 MV cm^{-1}) was recently reported.[28] The subthreshold swing of the pentacene TFT was not affected by the bias stress. When the pentacene TFT was left to relax for 40 min, V_{th} returned to its original value, indicating a relatively quick release of the trapped carriers. Figure 3a shows the transfer characteristics of a flexible DNTT TFT before and after 24 h of continuous bias stress with a gate–source voltage of −3 V (about 5.5 MV cm^{-1}), and Figure 3b shows the change in drain current during bias stress. After 24 h of bias stress, the drain current had dropped to 75% of its initial value, which is similar to the current drop in back-channel-etched amorphous silicon TFTs stressed with a gate field of 0.25 MV cm^{-1}.[26] Depending on the definition of V_{th}, the stress-induced V_{th} shift in the DNTT TFTs after 24 h is

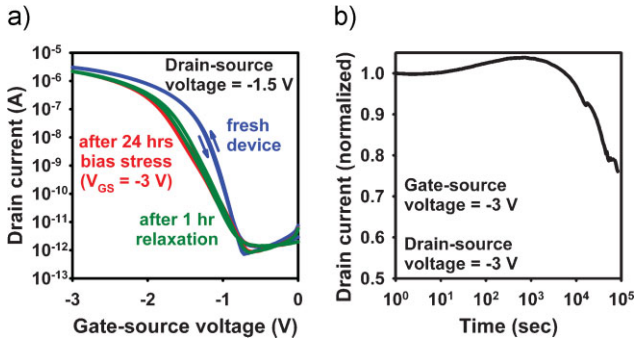

Figure 3. Bias-stress effect in a DNTT TFT on a flexible PEN substrate. The TFT was stressed continuously for 24 h with a gate–source voltage of −3 V and a drain–source voltage of −3 V. a) Transfer characteristics of the TFT measured before and after bias stress and after 1 h of relaxation. (The transfer characteristics were measured with a drain–source voltage of −1.5 V.) b) Drain current of the TFT as a function of time during bias stress.

0.12 V (if V_{th} is defined as the gate–source voltage at which the drain current is 10^{-10} A [27,28]) or 0.35 V (if V_{th} is defined as the intersect of the square-root of drain current curve with the gate–source voltage axis[29]). While the V_{th} shift in the DNTT TFTs is similar to that in pentacene TFTs,[28] there are two important differences: in the DNTT TFTs, the bias stress causes an increase in subthreshold swing (from 100 to 190 mV per decade), and neither V_{th} nor the subthreshold swing return to their original values after bias stress. Figure 3a shows the transfer characteristics of the same DNTT TFT after the stressed device had been left to relax for 1 h. The characteristics indicate no recovery of V_{th} and subthreshold swing, and measurements after several days also showed no recovery. This indicates that in the DNTT TFTs the energy required to release the carriers trapped during bias stress is substantially larger than in the pentacene TFTs. Further experiments will be necessary to determine whether this is related to the larger ionization potential of DNTT compared with pentacene.

In addition to the shelf-life and electrical stability of individual DNTT TFTs, we also investigated the performance and stability of logic circuits based on DNTT TFTs on flexible PEN. Figure 4 shows the circuit schematic and the transfer characteristics of a unipolar inverter with saturated load. The inverter characteristics were measured in air shortly after fabrication (Fig. 4a) and again after 8 months (Fig. 4b). As can be seen, the aged circuit still shows the correct logic function. Due to the time-dependent degradation in carrier mobility, the inverter transfer curves are slightly shifted toward more positive output voltages, and the maximum small-signal gain is reduced from 2.3 to 1.9.

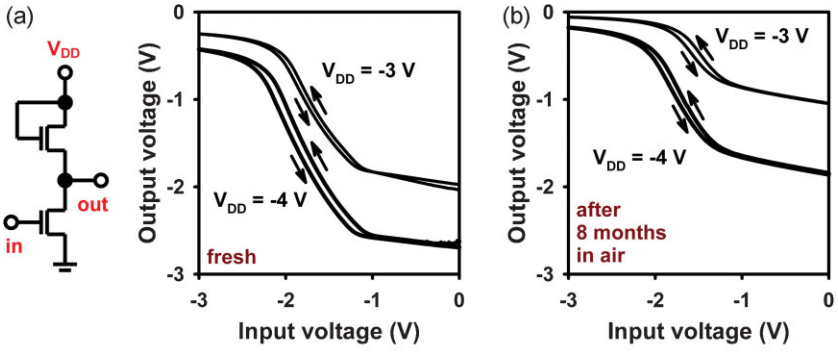

Figure 4. Schematic and transfer characteristics of an inverter with saturated load based on DNTT TFTs on a flexible PEN substrate. a) Inverter characteristics recorded shortly after device fabrication. b) Inverter characteristics recorded after 8 months in air. The drive TFT has a channel length of 10 μm and a channel width of 100 μm and the load TFT has a channel length of 50 μm and a channel width of 50 μm.

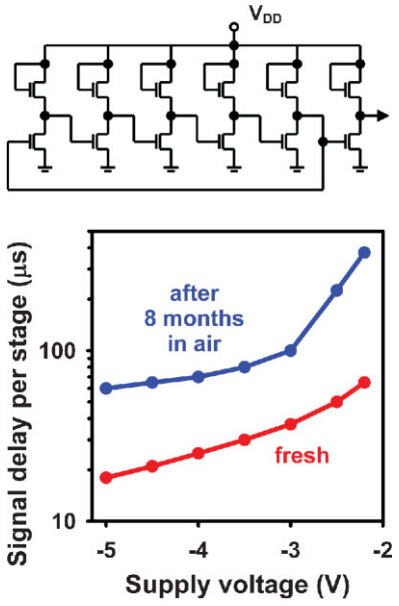

Figure 5. Circuit schematic and signal propagation delay per stage as a function of supply voltage of a 5-stage ring oscillator based on saturated-load inverters with DNTT TFTs on a flexible PEN substrate. Data measured shortly after device fabrication are shown in red; data recorded after 8 months in air are shown in blue. For all inverters, the drive TFT has a channel length of 10 μm and a channel width of 100 μm, and the load TFT has a channel length and width of 50 μm.

The dynamic performance of the flexible low-voltage DNTT TFTs was evaluated with a 5-stage ring oscillator based on saturated-load inverters. The drive TFTs have a channel length of 10 μm and a channel width of 100 μm. Owing to the large capacitance of the gate dielectric, the ring oscillators operate with a supply voltage as low as 2.2 V; to our knowledge these are the first flexible organic circuits that operate in ambient air with a supply voltage below 5 V. Figure 5 shows the signal propagation delay per stage as a function of supply voltage, measured shortly after fabrication (red curve) and measured again after the substrate had been stored in air for 8 months (blue curve). The stage delay measured at a supply voltage of −3 V (−5 V) is initially 37 μs (18 μs) and increases to 100 μs (60 μs) after 8 months. This increase in signal delay is approximately as expected based on the observed reduction in TFT mobility. For comparison, pentacene ring oscillators based on the same technology have a signal delay of 500 μs (at −3 V) and 200 μs (at

−5 V).[17] This means that after 8 months of storage in air the DNTT circuit is still several times faster than the pentacene circuit immediately after fabrication (while the latter degrades by several orders of magnitude during this time span).[17] In terms of practical applications this means that DNTT not only provides a substantial improvement in switching speed over pentacene, but also significantly reduces or even eliminates the need to develop and implement reliable encapsulation methods to protect the transistors and circuits from ambient air.

In terms of air stability, the DNTT devices and circuits represent a significant advancement over pentacene-based electronics. We believe that the better air stability of the DNTT TFTs in comparison to pentacene TFTs is related to the larger ionization potential of DNTT (5.4 eV) compared with that of pentacene (5.0 eV), since it is generally believed that a larger ionization potential leads to better stability against oxidation.[9–21] Alternatively, structural and morphological aspects have also been invoked to explain differences in air stability between organic semiconductors. For example, Katz et al. have hypothesized that a greater packing density in the solid state might reduce the probability of air-born oxidizing species penetrating the semiconductor film and reaching the buried TFT channel, which would explain differences observed in the air stability between organic TFTs based on different conjugated semiconductors having similar electrochemical potentials.[30] Although we cannot entirely rule out that the better air stability of the DNTT TFTs reported here is related to differences in thin-film morphology, we note that the packing density of DNTT is very similar to (if not slightly smaller than) that of pentacene (lattice parameters of DNTT:[22] $a = 6.187$ Å, $b = 7.662$ Å, $c = 16.21$ Å, $V = 767.7$ Å^3; lattice parameters of pentacene:[31] $a = 5.958$ Å, $b = 7.596$ Å, $c = 15.61$ Å, $V = 697$ Å^3). We also note that atomic force microscopy (AFM) images of thin films of DNTT and pentacene do not reveal any differences in thin-film microstructure that would explain the substantial difference in air stability (see Supporting Information). In contrast, the difference in ionization potential is substantial, so we believe this is the main reason for the difference in air stability.

In summary, we have manufactured and characterized flexible low-voltage thin-film transistors and integrated circuits based on DNTT, a conjugated organic semiconductor with a large ionization potential (5.4 eV) and a thin-film microstructure that favors efficient charge transport. The TFTs have a mobility of 0.6 cm^2 V^{-1} s^{-1}, and the ring oscillators have a signal delay of 18 μs per stage at a supply voltage of −5 V. Due to the excellent air stability of the semiconductor, the DNTT devices and circuits maintain about 50% of their initial performance for a period of 8 months of continuous exposure to ambient air.

Acknowledgements

The authors thank Benjamin Stuhlhofer at the Max Planck Institute for Solid State Research for expert technical assistance and Richard Rook at CADiLAC Laser for providing high-quality shadow masks. We gratefully acknowledge financial support provided by the New Energy and Industrial Technology Development Organization (NEDO) of Japan. Supporting Information is available online from Wiley InterScience or from the author.

Received: August 11, 2009
Published online: December 8, 2009

[1] F. De Angelis, M. Gaspari, A. Procopio, G. Cuda, E. Di Fabrizio, *Chem. Phys. Lett.* **2009**, *468*, 193.
[2] K. Takimiya, T. Yamamoto, H. Ebata, T. Izawa, *Sci. Technol. Adv. Mater.* **2007**, *8*, 273.
[3] M. Winkler, K. N. Houk, *J. Am. Chem. Soc.* **2007**, *129*, 1805.
[4] O. D. Jurchescu, J. Baas, T. T. M. Palstra, *Appl. Phys. Lett.* **2004**, *84*, 3061.
[5] J. H. Lee, G. H. Kim, S. H. Kim, S. C. Lim, Y. S. Yang, J. H. Youk, J. Jang, T. Zyung, *Synth. Metals* **2004**, *143*, 21.
[6] W. J. Kim, W. H. Koo, S. J. Jo, C. S. Kim, H. K. Baik, J. Lee, S. Im, *J. Vac. Sci. Technol, B* **2005**, *23*, 2357.
[7] S. H. Han, J. H. Kim, J. Jang, S. M. Cho, M. H. Oh, S. H. Lee, D. J. Choo, *Appl. Phys. Lett.* **2006**, *88*, 073519.
[8] H. Jung, T. Lim, Y. Choi, M. Yi, J. Won, S. Pyo, *Appl. Phys. Lett.* **2008**, *92*, 163504.
[9] H. Meng, Z. Bao, A. J. Lovinger, B. C. Wang, A. M. Mujsce, *J. Am. Chem. Soc.* **2001**, *123*, 9214.
[10] S. A. Ponomarenko, S. Kirchmeyer, M. Halik, H. Klauk, U. Zschieschang, G. Schmid, A. Karbach, D. Drechsler, N. M. Alpatova, *Synth. Metals* **2005**, *149*, 231.
[11] J. A. Merlo, C. R. Newman, C. P. Gerlach, T. W. Kelley, D. V. Muyres, S. E. Fritz, M. F. Toney, C. D. Frisbie, *J. Am. Chem. Soc.* **2005**, *127*, 3997.
[12] S. A. Ponomarenko, S. Kirchmeyer, A. Elschner, N. M. Alpatova, M. Halik, H. Klauk, U. Zschieschang, G. Schmid, *Chem. Mater.* **2006**, *18*, 579.
[13] J. Locklin, M. M. Ling, A. Sung, M. E. Roberts, Z. Bao, *Adv. Mater.* **2006**, *18*, 2989.
[14] M. Koppe, M. Scharber, C. Brabec, W. Duffy, M. Heeney, I. McCulloch, *Adv. Funct. Mater.* **2007**, *17*, 1371.
[15] T. Ashimine, T. Yasuda, M. Saito, H. Nakamura, T. Tsutsui, *Jpn. J. Appl. Phys.* **2008**, *47*, 1760.
[16] H. Meng, F. Sun, M. B. Goldfinger, F. Gao, D. J. Londono, W. J. Marshal, G. S. Blackman, K. D. Dobbs, D. E. Keys, *J. Am. Chem. Soc.* **2006**, *128*, 9304.
[17] H. Klauk, U. Zschieschang, R. T. Weitz, H. Meng, F. Sun, G. Nunes, D. E. Keys, C. R. Fincher, Z. Xiang, *Adv. Mater.* **2007**, *19*, 3882.
[18] K. Takimiya, H. Ebata, K. Sakamoto, T. Izawa, T. Otsubo, Y. Kunugi, *J. Am. Chem. Soc.* **2006**, *128*, 12604.
[19] H. Ebata, T. Izawa, E. Miyazaki, K. Takimiya, M. Ikeda, H. Kuwabara, T. Yui, *J. Am. Chem. Soc.* **2007**, *129*, 15732.
[20] T. Izawa, E. Miyazaki, K. Takimiya, *Adv. Mater.* **2008**, *20*, 3388.
[21] M. Kano, T. Minari, K. Tsukagoshi, *Appl. Phys. Lett.* **2009**, *94*, 143304.
[22] T. Yamamoto, K. Takimiya, *J. Am. Chem. Soc.* **2007**, *129*, 2224.
[23] H. Klauk, U. Zschieschang, J. Pflaum, M. Halik, *Nature* **2007**, *445*, 745.
[24] R. Libsch, J. Kanicki, *Appl. Phys. Lett.* **1993**, *62*, 1286.
[25] D. Knipp, R. A. Street, A. Völkel, J. Ho, *J. Appl. Phys.* **2003**, *93*, 347.
[26] B. Hekmatshoar, K. H. Cherenack, A. Z. Kattamis, K. Long, S. Wagner, J. C. Sturm, *Appl. Phys. Lett.* **2008**, *93*, 032103.
[27] K. H. Cherenack, A. Z. Kattamis, B. Hekmatshoar, J. C. Sturm, S. Wagner, *IEEE Electr. Dev. Lett.* **2007**, *28*, 1004.
[28] U. Zschieschang, R. T. Weitz, K. Kern, H. Klauk, *Appl. Phys., A* **2009**, *95*, 139.
[29] G. Horowitz, X. Peng, D. Fichou, F. Garnier, *J. Appl. Phys.* **1990**, *67*, 528.
[30] H. E. Katz, J. Johnson, A. J. Lovinger, W. Li, *J. Am. Chem. Soc.* **2000**, *122*, 7787.
[31] S. Schiefer, M. Huth, A. Dobrinevski, B. Nickel, *J. Am. Chem. Soc.* **2007**, *129*, 10316.

Supporting Information

Flexible Low-Voltage Organic Transistors and Circuits Based on a High-Mobility Organic Semiconductor with Good Air Stability

By *Ute Zschieschang, Frederik Ante, Tatsuya Yamamoto, Kazuo Takimiya, Hirokazu Kuwabara, Masaaki Ikeda, Tsuyoshi Sekitani, Takao Someya, Klaus Kern,* and *Hagen Klauk*

Figure on next page:

Atomic force microscopy (AFM) images of DNTT and pentacene films with an average thickness of 30 nm deposited by sublimation in a vacuum evaporator onto silicon substrates covered with a 20 nm thick layer of evaporated aluminum, a 3.6 nm thick layer of oxygen-plasma-grown aluminum oxide, and a 1.7 nm thick self-assembled monolayer of n-tetradecylphosphonic acid. During the deposition of the DNTT and pentacene films the substrates held at a temperature of 60 °C.

The AFM analysis does not reveal any differences in thin-film microstructure that would explain the substantial difference in air stability.

Image key:

Top left image: Topography, area 5 × 5 μm^2
Top right image: Amplitude, area 5 × 5 μm^2
Bottom left image: Height profile, distance 5 µm
Bottom right image: Amplitude, area 2 × 2 μm^2

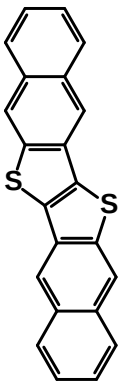

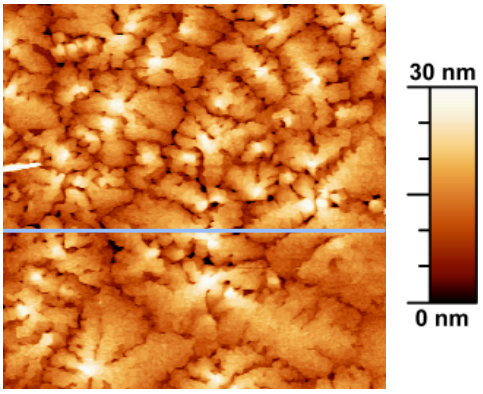

5 × 5 μm^2

5 × 5 μm^2

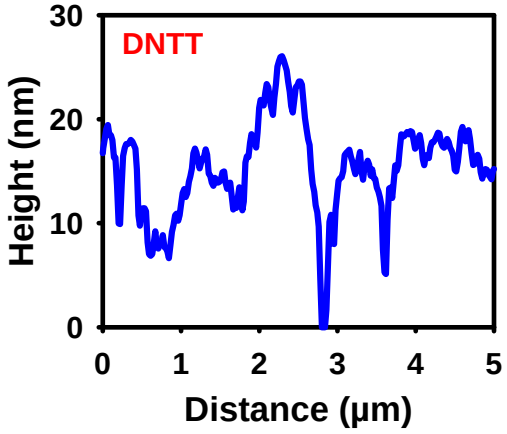

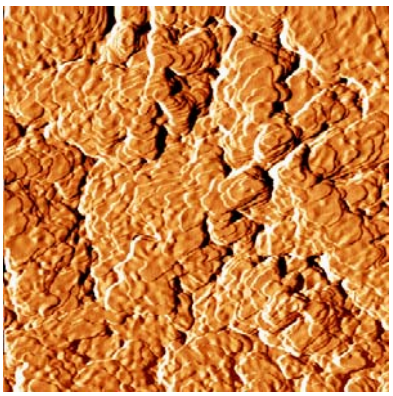

2 × 2 μm^2

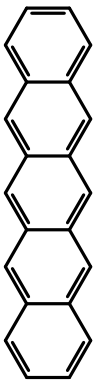

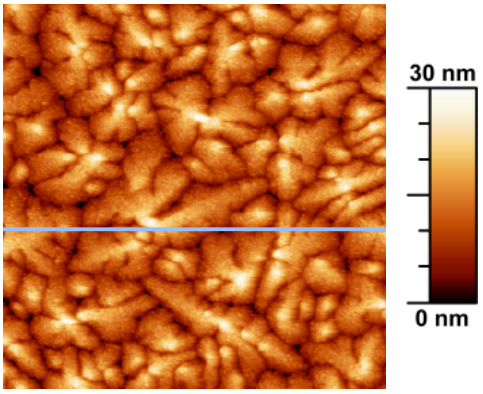

5 × 5 μm^2

5 × 5 μm^2

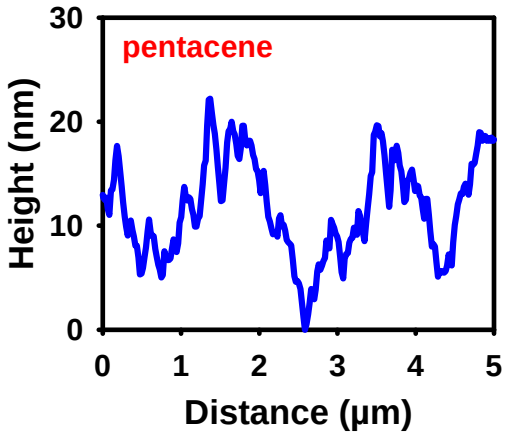

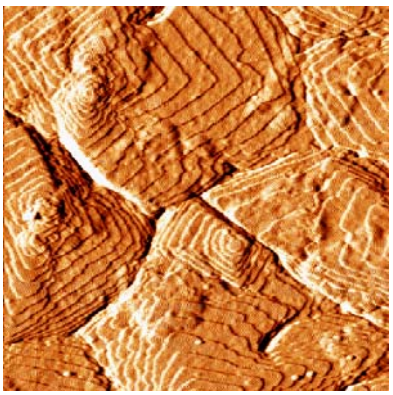

2 × 2 μm^2